Bayesian assimilation of rainfall sensors with fundamentally different integration characteristics

Andreas Scheidegger, Jörg Rieckermann**
**Eawag, The Swiss Federal Institute of Aquatic Science & Technology*

Abstract

Many sensors provide integrated (averaged) measurements of rain intensity. Although this integration is fundamental and can be different over time and/or space dimension(s), current approaches to assimilate rainfall signals do not take it into account. In this paper, we address this problem by a statistical approach to reconstruct rainfall fields that explicitly takes into account the different sensor integration characteristics. By applying a Gaussian process in a Bayesian framework, we provide a computationally efficient solution which is near real-time capable. A major advantage is that sensor signals with different scales (e.g. continuous, binary) and irregular time-intervals can be considered, which opens up great potential to use a multitude of novel rainfall sensors from telecommunication networks or building automation. This is first demonstrated on a didactical one-dimensional example. Second, real signals from rain gauges, precipitation radar and microwave links are assimilated for a small urban area of 3km^2 in Switzerland. Both examples suggest that the explicit consideration of the integration characteristics enables the reconstruction of spatial details smaller than radar pixels.

Introduction

The need for high resolution rain maps of small sensitive areas led to the development of sensors with new measurement principles, such as micro wave links (MWL) (Atlas & Ulbrich, 1977), modified marine radars (Rasmussen et al., 2008), simple acoustic rain gauges (Nystuen, 1999), and even sensors of automatic car windshield wipers (Haberlandt & Sester, 2010; Rabiei et al., 2013). Many of these new sensors are inexpensive or based on existing infrastructures. This makes them ideal to complement weather radars and rain gauges to enable better rain field reconstructions.

In principal, every additional unbiased measurement should improve the knowledge about the current rain field. However, different sensors may measure fundamentally different properties of the rain field and a statistical assimilation technique should consider this. For example, tipping buckets observe point rain intensities but with variable temporal integration. In contrast, operational rainfall radar products in Cartesian coordinates provide information about the average intensity of the area covered by a pixel, and MWLs provide path-integrated estimates along the link. A large number of methods have been proposed to assimilate radar and rain gauge measurements (e.g. Todini, 1999; Goudenhoofdt & Delobbe, 2009; Erdin et al., 2012; Sideris et al., 2013). However, to the best of our knowledge, different integration behaviors of sensors have not been explicitly considered so far. Only path-integration of MWL signals has been taken into account (Grum et al., 2005; Zinevich et al., 2008; Goldshtein et al., 2009; Bianchi et al., 2013). Furthermore, as far we know only Grum et al. (2005) and Bianchi et al. (2013) attempted to assimilate signals from more than two sensors types: gauges, radar and MWL.

In this this paper, we therefore advocate for an assimilation approach that explicitly considers the integration in time and/or space of every sensor. We avoid a discretization of the integration domains by an analytical solution, which enables an efficient computation. In addition to the different measurement characteristics, our approach can handle sensors signals with any scale (e.g., continuous, binary). For the first time, this makes it possible to realistically describe novel, unconventional sensors in a statistically rigorous manner. This generic assimilation method enables us to assess the benefits of unconventional sensors and their optimal placement. Last but not least, our approach is formulated continuously in time and space, which facilitates consideration of signals with irregular time intervals between measurements. The remainder of this manuscript is as follows: In the next section we present the assimilation approach. Then, we demonstrate the effect of integrating sensors on a first didactical example by reconstructing point rainfall intensities over time. In the second example we assimilate the signals of five rain gauges, three MWLs and 20 radar pixels for a small urban catchment. Finally, we discuss the most important points and draw our final conclusions.

Method

In general, two sources of information about a rain field are available that a data assimilation approach could consider: i) prior knowledge on the regional rainfall characteristics and ii) sensor signals (including an estimate of their observation errors).

The prior knowledge reflects the typical behavior of rain fields but does not contain information about the current situation. For example, an important prior knowledge is that rain fields show a strong temporal and spatial correlation; it is likely that at two nearby points the intensities are similar.

Sensors taking direct or indirect measurements of the rain field provide information about the current situation and are used to update the prior knowledge. Depending on type and location of a sensor, different properties of the rain field are measured. In the following, “sensor” does not only refer to a physical measurement device, but to any source of rain related signals. For example, the operator of a tipping bucket rain gauge may only provide hourly rain amounts. Similarly, in most cases the rain map produced from an operational rain radar is regarded as a sensor signal rather than the raw signal of the radar.

In the following, first the characterizations of the sensors and the prior knowledge are described. Then it is explained how the prior knowledge is updated by assimilating sensors signals.

Sensor characterization

Different sensor types observe different properties of the rain field. As such, they may provide signals with different resolutions and scales, and differ in accuracy. These characteristics are represented by the *signal distribution* of a sensor (sometimes also called ``observation model'').

In the simplest case, a sensor measures instantaneous point rainfall intensities at a coordinate $C = [x, y, t]$ (x, y are the spatial and t the temporal dimension). Another class of sensors measures *integrated* intensities. For example non-recording Standard Rain Gauges, as used by the U.S. National Weather Service, integrate over time and deliver, for example, daily rainfall sums. Accordingly, the (processed) signals from operational weather radars represent rain intensities integrated (averaged) over the area of a pixel and MWLs measure the path-average intensity.

The signal distribution is the probability density distribution of the signal (or the probability mass function for discrete signals), given either on the intensity R_C at a point C or on the intensity integrated over a domain D, $\bar{R}_D = \int_D R_{C(v)} dv$. The extent of the domain D can be in temporal and/or spatial dimension(s). The signal distribution of a sensor is written as

$$p_S(S|P_S)$$

where P_S, depending on the signal, is either a point or integrated intensity.

We impose no other restrictions on the sensor distribution. For example the distribution might be continuous, discrete (includes binary signals), or even qualitative (e.g. ``no rain'', ``light rain'', ``heavy rain''). This makes it possible to describe many different sensors.

Prior knowledge

The prior knowledge of the rain field is modeled with a Gaussian process (GP) with a three-dimensional input space (x, y, t). A GP is usually defined by a mean function $m(C)$ and a co-variance function $k(C, C')$. These functions are selected so that the GP reflects the prior knowledge.

For small areas a constant will be sufficient as mean function. The choice of the covariance functions, however, has a great influence on the behavior of the GP. For a first attempt we used a simple formulation that considers temporal and spatial correlation:

$$cov(R_C, R_{C'}) = k(C, C') = \sigma^2 exp\left[-\left(\frac{|t-t'|}{l_{temp}}\right)^p - \left(\frac{d}{l_{spatial}}\right)^p\right], \quad \text{with } 0 \leq p \leq 2 \qquad (1)$$

where d is the spatial distance, $\sqrt{(x-x')^2 + (y-y')^2}$. The standard deviation of the process is defined by σ, temporal and spatial correlation length is controlled by l_{temp} and $l_{spatial}$, and p influences the “smoothness” of the process.

Let $\mathcal{R}$ denote a set of rain intensities at different locations in time/space. Further, $p(\mathcal{R})$ is the joint probability density function (pdf) of the GP of all intensities of $\mathcal{R}$. Similar, $p(\mathcal{R}|\mathcal{R}')$ is the pdf of all elements of $\mathcal{R}$ conditioned on the intensities of set $\mathcal{R}'$.

A well-known and important property of the GP is that $p(\mathcal{R})$ and $p(\mathcal{R}|\mathcal{R}')$ can be computed analytically based on the mean and covariance function (see e.g. Rasmussen & Williams, 2006). However, because of the integrating sensors we also want to consider the possibility that a set $\mathcal{R}$ contains integrated intensities ($\bar{R}_D$). An analytical solution to compute a distribution conditioned on integrated intensities is crucial for the efficient assimilation of integrating sensors.

The key point is the fact that an integral of a GP is normal distributed. Therefore, if mean and covariance of the integral are known, the standard equations for multivariate normal distributions can be used to compute $p(\mathcal{R})$ and $p(\mathcal{R}|\mathcal{R}')$ even if set $\mathcal{R}$ or $\mathcal{R}'$ contain integrated intensities.

The mean of an integrated intensity, $\bar{R}_D = \int_D R_{C(v)} dv$, is given by

$$E(\bar{R}_D) = \int_D m(v) dv, \qquad (2)$$

the covariance of $\bar{R}_D$ and the rain intensity at a point C (R_C), or another integrated intensity, is derived from $k(C, C')$:

$$cov(\bar{R}_D, R_C) = \int_D k(C, v) dv\ , \quad cov(\bar{R}_{D^1}, \bar{R}_{D^2}) = \iint_{D^1, D^2} k(v, w) dv\, dw\ . \qquad (3)-(4)$$

With this equations the covariance matrix of a set $\mathcal{R}$ can be computed even if it includes integrated intensities.

Bayesian Assimilation

Concept

The assimilation of the signals is based on Bayesian updating and can be written in two steps: i) calibration (or "conditioning"), and ii) interpolation (or "prediction").

All available signals are contained in set $\mathcal{S}$, and all points or domains which are measured by a signal of $\mathcal{S}$ are elements of $\mathcal{R}^S$. The calibration step is then the application of the Bayes theorem to compute the posterior distribution of $\mathcal{R}^S$, i.e. the distribution of the rain intensities conditioned on the measured signals

$$p(\mathcal{R}^S|\mathcal{S}) \propto p(\mathcal{R}^S) \prod_{S \in \mathcal{S}} p_S(S|P_S)\ . \qquad (5)$$

The intensities of the points and domains of $\mathcal{R}^S$ are not of interest per se. However, the result of eq(5) can be used to calculate the predictive distribution of any arbitrary set. To construct rain maps, usually the intensities at points on a grid are wanted. If $\mathcal{R}^p$ is the set of the points of interest for predictions, its distribution is

$$p(\mathcal{R}^p|\mathcal{S}) = \int p(\mathcal{R}^p|\mathcal{R}^S) p(\mathcal{R}^S|\mathcal{S})\, d\mathcal{R}^S \qquad (6)$$

where $p(\mathcal{R}^p|\mathcal{R}^S)$ is based on the prior and $p(\mathcal{R}^S|\mathcal{S})$ is obtained by eq(5). The result of the assimilation is the distribution of rain intensity at any point contained in $\mathcal{R}^p$ under consideration of all available signals.

Numerical implementation

In most cases the desired distribution $p(\mathcal{R}^p|\mathcal{S})$ cannot be computed analytically.[1] Instead the aim is to obtain a sample from it with Monte Carlo algorithms. Based on a sample, summary statistics such as mean, standard deviations, etc. can be calculated. The sampling is done in steps: first a sample of $p(\mathcal{R}^S|\mathcal{S})$ is obtained, that then enables the generation of a sample from $p(\mathcal{R}^p, \mathcal{R}^S|\mathcal{S})$ in a second step. The marginalization over $\mathcal{R}^S$ as shown in eq(6) is trivial. Given a sample of a joint distribution, any marginal distribution can be obtained by ignoring the samples of the other dimensions.

To sample from eq(5) we implemented an adaptive Metropolis-within-Gibbs sampler proposed by Roberts and Rosenthal (2009) because the "full conditionals" can be computed efficiently. As $\mathcal{R}^S$ contains much less elements (typically one per measurement) than $\mathcal{R}^p$, this step is relatively fast. In the second step, it is easy to sample from $p(\mathcal{R}^p, \mathcal{R}^S|\mathcal{S})$, because

[1] If all sensors do not integrate and their distributions are normal and linear, the approach is similar to Kriging and can be solved analytically.

$p(\mathcal{R}^p|\mathcal{R}^S)$ is a multivariate normal distribution. Nevertheless, the calculation of the covariance matrix may require many numerical integrations because of eq(2) – (4).

The assimilation procedure is implemented with *Julia* (Bezanson et al., 2012), a relatively new high-level program language designed for scientific computing and a performance comparable to compiled languages. The rain maps were produced with *R* (R Development Core Team, 2014).

Examples

One-dimensional example

A signal of integrating sensors, such as mentioned above, only provides information about the average intensity in the measured domain. However, in the following didactical example, we will demonstrate how the spatial/temporal distribution of the rain intensities within the integration domain can still be reconstructed, given that additional signals are available. For better illustration, we assume that only the rain intensity over time at one location is of interest. Also, we use artificial signals from only two different sensors. Sensor A provides a binary signal ("above" or "below" threshold), similar as sensors used in building automation. Sensor B measures the intensity integrated over a time period, such as a tipping bucket rain gauge. To emphasize the effect of the assimilation, we assume no observation error for both sensors. A relatively uncertain prior is assumed that expects some rain in this period of time.

First, we only assimilate sensor A, which observes "below threshold", and the prior (Figure 1a). The effect of the signal is small as it changed the mean of the predictive distribution only slightly. In this situation the signal most probably has not much value. Second, we assimilate only sensor B, which observes on average more rainfall than sensor A's threshold, and the prior (Figure 1b). In contrast to Sensor A, Sensor B's signal shifts the mean considerably. Third, we use both signals, together with the prior, in the assimilation (Figure 1c). Now the binary signal has a strong influence: it indicates that the higher intensities happened more likely in the second half of the integration period of Sensor B.

This example shows that even an apparently poor signal may provide important information in combination with other signals. Therefore assessing the information value of a single signal in isolation is difficult. For this reason all signals should be assimilated in practical applications.

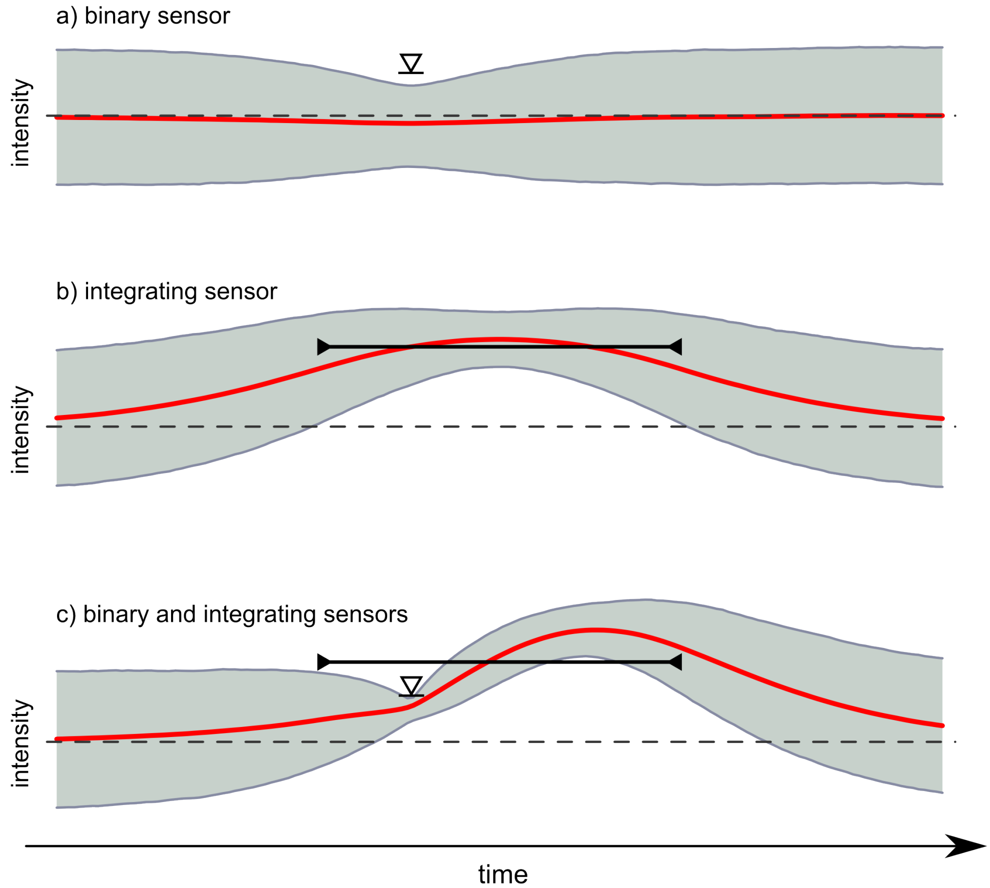

Figure 1: One-dimensional example of the assimilation of a binary and an integrating sensor. The red curve represents the mean of the predictive distribution after assimilation, the gray area its 90%-credibility region. The signal of the binary sensors provides only the information that the intensity is below a certain level (a). The integrating sensor measures the average intensity over the time-span indicated by the black line in b). In c) the assimilation of both sensors is shown.

Assimilation of real signals

The approach was applied to assimilate signals measured in Adliswil, Switzerland. The urban catchment has an area of about 3 km^2 for which accurate rain maps are desired (Fu, 2013). For this purpose five rain gauges were installed in the catchment an operated for 8 months. Additionally, data of three nearby commercial MWL's are available (length 2.2km, 38GHz; 3km, 38GHz; 6.3km, 23GHz; all with horizontal polarization). The catchment and the surrounding area are covered by 20 pixels of the Swiss operational weather radar product PRECIP-SV (1km spatial, 180sec temporal resolution) produced by Meteoswiss (Germann et al., 2006). These 20 pixels of the radar rain map were considered as sensors with spatial integration. For this example we assumed a relative standard deviation of 15% (gauges), 30% (MWLs), and 50% (radar) for the signal distribution. The temporal correlation length for the prior was derived from a long rain series measured by a gauge and the spatial correlation length is based on the observations of Bianchi et al. (2013).

The rain field that was reconstructed from the prior and the five gauges, scenario A, is shown in Figure 2a. For Figure 2b three MLW signals were additionally assimilated (scenario B). With these additional signals the extend of the rain cell in the north-west is more clearly defined. The corresponding uncertainty (shown in Figure 2d) is lowest at the location of the gauges. The MLWs reduce the uncertainty less, because they provide merely information about the average intensity along a path. Finally, Figure 2c shows the result of assimilating all signals of gauges, MLWs and, radar (scenario C). The radar provides further information about the spatial distribution. With the other signals details within the radar pixels could be reconstructed. As the radar measured considerably less rainfall than the other sensors, the maximum intensity is reduced. However, recent investigations of Fu (2013) suggest that radar measurements systematically underestimate rain intensities in the area of this catchment. Therefore a correction of the radar signal may be beneficial.

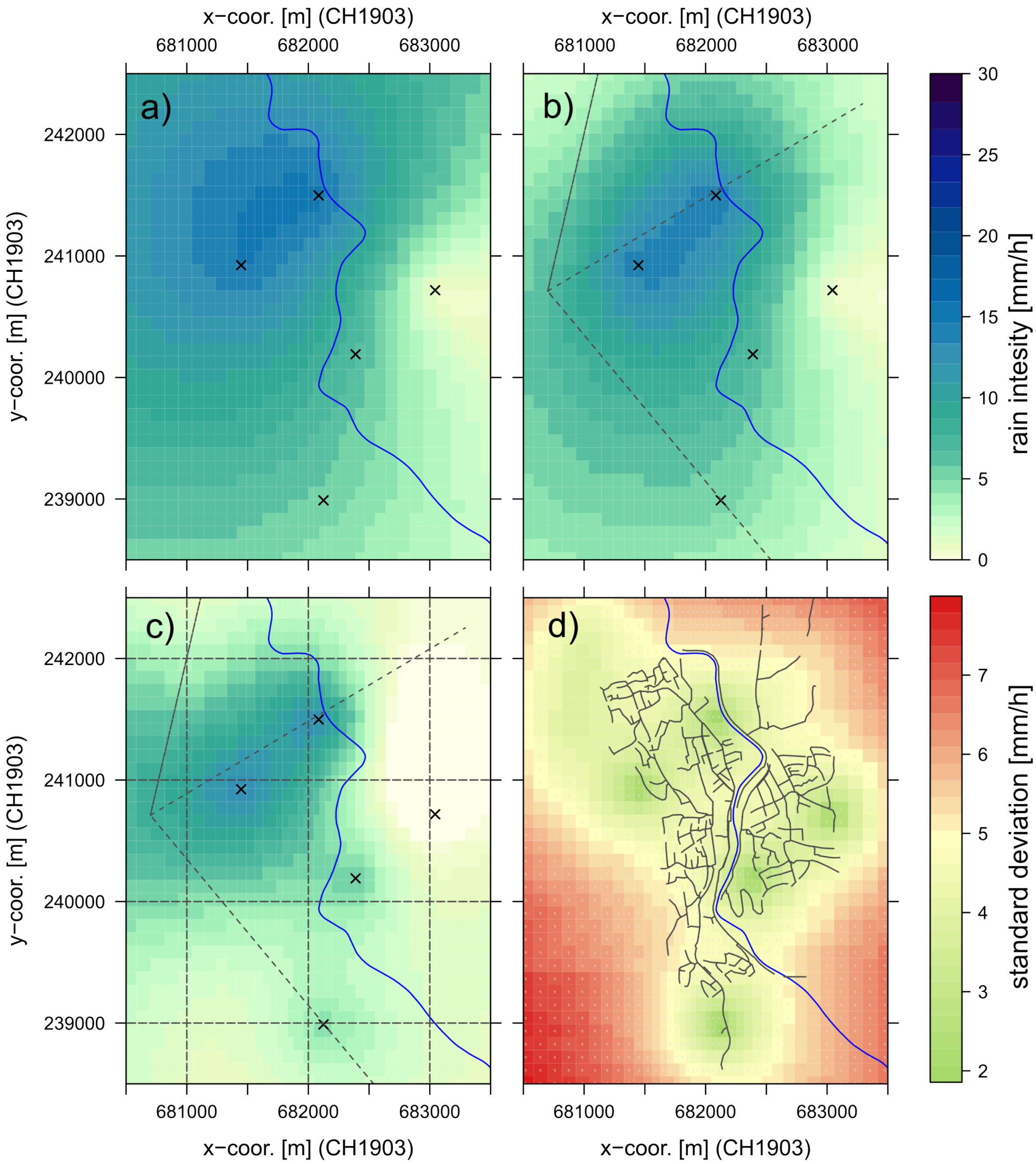

Figure 2: Rain intensities reconstructed at 1600 points by assimilating different signals measured in the catchment of Adliswil, Switzerland at 09-06-2013 21:32:30. The mean of the predictive distribution is shown. The river Sihl is marked by the blue line. The assimilation of 5 rain gauges (x) is shown in a). In b) additionally the signals of the tree MWLs (dashed lines) are used. The result of considering additionally the surrounding radar pixels (dashed lines) is shown in c). The uncertainty expressed as standard deviation of the predictive distribution for the result in b) is shown in d) together with the drainage system of Adliswil (gray lines).

Discussion and conclusions

We presented a flexible Bayesian assimilation approach to reconstruct rain fields based on signals from fundamentally different sensors. The main innovation is that the integration-characteristic of each sensor is considered and the computational costs are kept low at the same time. As demonstrated by the first example, the combination of integrating sensors and other signals makes it possible to reconstruct details of the rain field within the measured domains (e.g. radar pixels). This is particularly important if high-resolution rain maps of small areas are computed, which may be covered by only few radar pixels.

Furthermore, the method requires no assumption about the distribution of the signals, such as normality or linearity. The continuous formulation without fixed time-steps enables a natural handling of sensors that record measurements in irregular intervals. This flexibility makes it possible to assimilate new, unconventional sensors and assess their information value in combination with existing signals.

We applied the approach in a realistic setting with signals of a measurement campaign in a small urban catchment. It was possible to reconstruct details of rain fields within the radar pixels and to provide uncertainty estimates. Even though Monte Carlo sampling is required, this example suggests that the computation of the assimilation is fast enough to enable a near real-time operation; the assimilation of 46 signals and predictions on 1600 points required roughly 100 seconds on a Intel i7, 2.8 GHz. A large fraction of the time is spent on the computation of the covariance matrix, which could be more optimized or even parallelized.

The approach has still some limitations. Currently the prior can only be expressed as Gaussian process. This is not satisfactory as rain intensities have a heavily skewed non-negative distribution. Usually, this is modeled with a transformation (e.g. Erdin et al., 2012). For the presented approach the implementation of a transformation is not trivial because the integral of a transformed GP is not Gaussian anymore—a property that enables an efficient computation. However, as the prior is usually not very informative and is quickly overwhelmed by the measured signals, the missing transformation is not so critical. Another challenge is to find the most suitable formulation of the covariance function. With more sophisticated formulations advection and diffusion could be modeled (Sigrist et al., 2012) or dependencies of external variables such as temperature or wind may be useful. Even though the method is very flexible regarding the signal distribution of the sensors, the characterization of a sensor is intrinsically challenging, as the true rain field can never be measured. This is, of course, true for all assimilation approaches.

We hope to introduce a suitable transformation in the next version to allow for more realistic prior formulations while keeping the computation efficient. Furthermore, a validation by means of cross-validation and an investigation of the predictive performance of different covariance formulations should be done. An interesting extension would be to use forecasts of numerical weather models as signals. In combination with measurements, this seems promising for short-term forecasts of the rain field.

We see the largest potential of this approach in urbanized areas, for example in the management and control of urban drainage systems. This requires real time rain information with high temporal and spatial resolution. Here, the incorporation of a large number of (novel) sensors is most promising. Our first results suggest that many simple sensors (e.g. binary) may be more beneficial than few precise ones. Given the emerging possibilities for wireless sensor networks and that high precision is not required, the construction of robust autonomous low-cost sensors appears to be feasible.

Development of new sensors to complement standard measurements are always welcome. Ideally, the data sheet of every novel sensor would include a description of its signal distribution. Having this, novel sensors could easily be included in a probabilistic assimilation framework. To benefit most of new sensors, however, generic methods to correctly assimilate the additional signals must be available.

All code is freely available on https://github.com/scheidan/CAIRS. Feedback is highly welcome.

Acknowledgements

We would like to thank Prof. H.R. Künsch of the Seminar for Statistics at ETHZ for the derivation of equation (2) – (4) and stimulating discussions.

References

Atlas, D., & C. W. Ulbrich, 1977. Path- and Area-Integrated Rainfall Measurement by Microwave Attenuation in the 1–3 cm Band. Journal of Applied Meteorology 16: 1322–1331.

Bezanson, J., S. Karpinski, V. B. Shah, & A. Edelman, 2012. Julia: A Fast Dynamic Language for Technical Computing. arXiv:1209.5145 [cs] , http://arxiv.org/abs/1209.5145.

Bianchi, B., P. J. van Leeuwen, R. J. Hogan, & A. Berne, 2013. A variational approach to retrieve rain rate by combining information from rain gauges, radars and microwave links. J. Hydrometeor .

Erdin, R., C. Frei, & H. R. Künsch, 2012. Data transformation and uncertainty in geostatistical combination of radar and rain gauges. Journal of Hydrometeorology 13: 1332–1346.

Fu, R., 2013. The effect of different rainfall information on sewer flow predictions. Master Thesis, ETHZ.

Germann, U., Galli, G., Boscacci, M., and Bolliger, M. (2006) Radar precipitation measurement in a mountainous region. Quarterly Journal of the Royal Meteorological Society, 132(618): 1669–1692.

Goldshtein, O., H. Messer, & A. Zinevich, 2009. Rain rate estimation using measurements from commercial telecommunications links. Signal Processing, IEEE Transactions on 57: 1616–1625.

Goudenhoofdt, E., & L. Delobbe, 2009. Evaluation of radar-gauge merging methods for quantitative precipitation estimates. Hydrol. Earth Syst. Sci. 13: 195–203.

Grum, M., S. Kraemer, H.-R. Verworn, & A. Redder, 2005. Combined use of point rain gauges, radar, microwave link and level measurements in urban hydrological modelling. Atmospheric Research 77: 313–321.

Haberlandt, U., & M. Sester, 2010. Areal rainfall estimation using moving cars as rain gauges – a modelling study. Hydrol. Earth Syst. Sci. 14: 1139–1151.

Nystuen, J. A., 1999. Relative Performance of Automatic Rain Gauges under Different Rainfall Conditions. Journal of Atmospheric and Oceanic Technology 16: 1025–1043.

R Development Core Team, 2014. R: A Language and Environment for Statistical Computing. Vienna, Austria, http://www.R-project.org/.

Rabiei, E., U. Haberlandt, M. Sester, & D. Fitzner, 2013. Rainfall estimation using moving cars as rain gauges – laboratory experiments. Hydrol. Earth Syst. Sci. 17: 4701–4712.

Rasmussen, C. E., & C. K. I. Williams, 2006. Gaussian processes for machine learning. MIT Press, Massachusett.

Rasmussen, M. R., S. Thorndahl, & K. Schaarup-Jensen, 2008. Vertical Pointing Weather Radar for Built-up Urban Areas. 11th International Conference on Urban Drainage. Edinburgh, UK, http://web.sbe.hw.ac.uk/staffprofiles/bdgsa/11th_International_Conference_on_Urban_Drainage_CD/ICUD08/pdfs/437.pdf.

Roberts, G. O., & J. S. Rosenthal, 2009. Examples of adaptive MCMC. Journal of Computational and Graphical Statistics 18: 349–367.

Sideris, I. V., M. Gabella, R. Erdin, & U. Germann, 2013. Real-time radar–rain-gauge merging using spatio-temporal co-kriging with external drift in the alpine terrain of Switzerland. Quarterly Journal of the Royal Meteorological Society n/a–n/a.

Sigrist, F., H. R. Künsch, & W. A. Stahel, 2012. A Dynamic Nonstationary Spatio-temporal Model for Short Term Prediction of Precipitation. The Annals of Applied Statistics 6: 1452–1477.

Todini, E., 1999. A Bayesian technique for conditioning radar precipitation estimates to rain-gauge measurements. Hydrol. Earth Syst. Sci. 5: 187–199.

Zinevich, A., P. Alpert, & H. Messer, 2008. Estimation of rainfall fields using commercial microwave communication networks of variable density. Advances in Water Resources 31: 1470–1480.